

UDC 541.136+546.34+544.463

## Structure and Electrochemical Properties of $\text{LiCo}_{1-y}\text{Fe}_y\text{PO}_4$ Solid Solutions as High-Voltage Cathode Materials for Lithium-Ion Rechargeable Cells \*

O. A. PODGORNOVA and N. V. KOSOVA

*Institute of Solid State Chemistry and Mechanochemistry, Siberian Branch of the Russian Academy of Sciences, Ul. Kutateladze 18, Novosibirsk 630128 (Russia)**E-mail: kosova@solid.nsc.ru*

### Abstract

Single-phase superfine  $\text{LiCo}_{1-y}\text{Fe}_y\text{PO}_4$  solid solutions were synthesized with the use of a mechanochemically stimulated carbothermal reduction of iron and cobalt oxides throughout the entire range of  $0 \leq y \leq 1$ . The mechanical activation was carried out using an AGO-2 planetary mill. According to the scanning electron microscopy, the average primary particle size of the samples synthesized ranges within 200–250 nm. According to the XRD phase analysis, all the samples crystallize in the orthorhombic system, with space group  $Pnma$ . The volume of the unit cell increases with increasing the content of iron in samples. According to Mössbauer (NGR) spectroscopy, all iron ions are in the oxidation state  $2+$  in an octahedral environment typical for olivine. Electrochemical properties of  $\text{Li}_{1-y}\text{Fe}_y\text{PO}_4$  were investigated by means of galvanostatic cycling. It has been demonstrated that with the increase of Fe content a marked shift in the potential of the  $\text{Co}^{2+}/\text{Co}^{3+}$  pair toward lower voltage values occurs, whereas the potential of the  $\text{Fe}^{2+}/\text{Fe}^{3+}$  pair remains almost unchanged.

**Key words:** lithium-ion rechargeable cells, cathode materials,  $\text{LiCo}_{1-y}\text{Fe}_y\text{PO}_4$ , mechanical activation, crystal structure, cycling

### INTRODUCTION

In the today's world, there is a growing demand for lithium-ion rechargeable cells (LIC). The scope of LIC is diverse; it covers almost all aspects in the life of the modern industrial society: production, everyday life and recreation services. The development of large-scale rechargeable cells for transport and for energy storages requires for further increasing capacity and power characteristics thereof, as well as improving their performance over a wide temperature range. This stimulates searching for novel electrode materials and developing new methods of their synthesis [1].

In recent years, much attention is paid to studying a new class of cathode materials, such

as lithium and a transition metal orthophosphates with the structure of olivine (space group  $Pnma$ ), that have a high operation voltage and a sufficiently high electrochemical capacity. Lithium iron phosphate  $\text{LiFePO}_4$  was first proposed as a cathode material in 1997 [2], while its industrial production began in 2010. Compound  $\text{LiFePO}_4$  is characterized by the operation voltage of 3.4 V, relatively to  $\text{Li}/\text{Li}^+$  pair, and specific energy value of  $578 \text{ W} \cdot \text{h/g}$ , marked by a high chemical, thermal and structural stability in the course of cycling, what makes it the most popular cathode material for the production of large-size batteries. The disadvantage of this material is a low electrical conductivity ( $\sigma \sim 10^{-9} \text{ S/cm}$ ), however, it is overcome by obtaining  $\text{LiFePO}_4$  in the nano-sized state, and surface modifying by highly conductive carbon [3].

In the series of structural analogues  $\text{LiFePO}_4$ – $\text{LiMnPO}_4$ – $\text{LiCoPO}_4$ – $\text{LiNiPO}_4$ , there is an in-

\* Materials of the IV Int. Meeting “Fundamentals of Mechanochemical Technologies”, June 25–28, 2013, Novosibirsk, Russia.

crease in the operation voltage observed, and, accordingly, the specific energy and power of the rechargeable cell exhibits an increase. So, for  $\text{LiCoPO}_4$  the voltage amounts to 4.8 V, whereas the specific energy value is equal to  $801 \text{ W} \cdot \text{h/g}$ , which is 1.5 times higher than the value for  $\text{LiFePO}_4$ . However  $\text{LiCoPO}_4$  exhibits an even lower electrical conductivity ( $\sigma \sim 10^{-15} \text{ S/cm}$ ), and the operation voltage thereof is beyond the electrochemical stability window for the standard electrolyte (4.8 V). A higher voltage results in the decomposition of the electrolyte and the interaction thereof with the cathode material. As the result, the cathode material undergoes a considerable degradation, and the rechargeable cell loses the capacity in the course of cycling [4].

It is demonstrated [3, 5, 6] that the preparation of  $\text{LiCoPO}_4$  in nanosized state, doping with the cations of other metals and making a highly conductive carbon coating with the use of a variety of carbon-containing precursors provides satisfactory performance of the cathode materials with respect to the electrical conductivity the cycling ability. Recently, the authors of [7] found that a partial substitution of  $\text{Mn}^{2+}$  ions by  $\text{Fe}^{2+}$  ions in  $\text{LiMnPO}_4$  causes the shift of the redox potential of the  $\text{Mn}^{2+}/\text{Mn}^{3+}$  couple to be shifted towards the region of lower voltage values. Similar studies are also under development for  $\text{LiCoPO}_4$  [8–11]. The shift of the redox potential of the  $\text{Co}^{2+}/\text{Co}^{3+}$  couple towards lower voltage values can significantly improve the electrochemical properties of  $\text{LiCoPO}_4$  due to decreasing the decomposition level of the electrolyte and degradation level of cathode material.

As a rule, highly dispersed cathode materials for LIC are prepared using solution methods (e. g., sol-gel [12], and hydrothermal technique [13]). However, in the course of realizing these methods, liquid wastes are formed, which requires for further recycling thereof. At the Institute of Solid State Chemistry and Mechanochemistry of the SB RAS (Novosibirsk) there is a modern environmentally friendly and energy-saving solid-state method for mechanical activation (MA) of solid-phase processes. According to the results of numerous studies, a preliminary MA of the mixture of initial reagents promotes a significant decrease in the temperature and in the subsequent annealing

time, thereby the uniformity of the final product could be improved, and the product itself could be obtained in a highly dispersed state [14].

The present work consisted in studying a solid-phase synthesis of  $\text{LiCo}_{1-y}\text{Fe}_y\text{PO}_4$  ( $0 \leq y \leq 1$ ) solid solutions with the use of mechanochemically stimulated carbothermal reduction of iron and cobalt oxides; crystal structure, local structure and electrochemical properties thereof were investigated.

## EXPERIMENTAL

The preliminary MA of the initial multi-component mixture of reagents such as  $\text{Li}_2\text{CO}_3$ ,  $\text{Co}_3\text{O}_4$ ,  $\text{Fe}_2\text{O}_3$ ,  $(\text{NH}_4)_2\text{HPO}_4$  and carbon was carried out using an AGO-2 planetary mill. The annealing of mechanically activated mixtures was performed under an inert atmosphere at  $750^\circ\text{C}$ . Excess carbon (2–3 %) was used in order to obtain an electronically conducting carbon coating.

The resulting samples were analyzed by means of X-ray diffraction (XRD), Mössbauer (NGR) spectroscopy, scanning electron microscopy (SEM) and galvanostatic cycling. The XRF studies were performed using a Bruker D8 Advance diffractometer ( $\text{CuK}_\alpha$  radiation, scanning pitch  $0.02^\circ/\text{s}$ ). Refining the lattice parameters by means of the Rietveld method was performed using a GSAS software package [15]. The NGR spectra were registered by means of

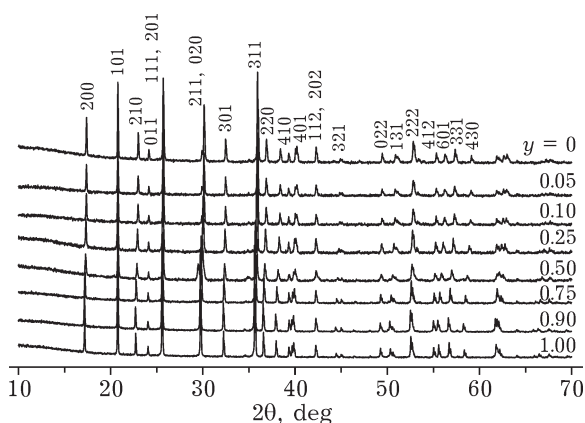


Fig. 1. Diffraction patterns of  $\text{LiCo}_{1-y}\text{Fe}_y\text{PO}_4$  ( $0 \leq y \leq 1$ ) solid solutions.

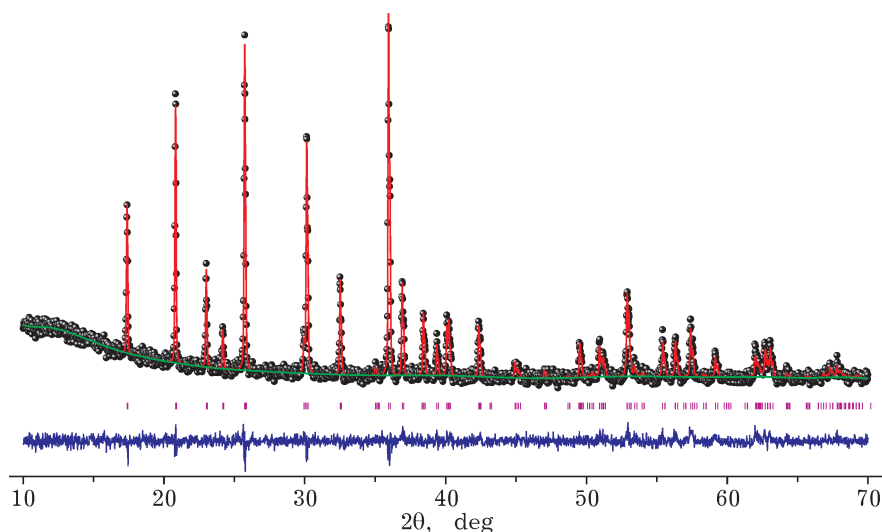


Fig. 2. Diffraction pattern of  $\text{LiCo}_{0.9}\text{Fe}_{0.1}\text{PO}_4$ , refined by means of Rietveld method.

a NZ-640 NGR spectrometer (Hungary) equipped with a  $^{57}\text{Co}$  radiation source. The particle size and morphology were examined by means of a Hitachi TM-1000 scanning electron microscope, whereas the EDX spectra were registered using a TM1000 EDS detector. The procedure of cycling was performed in a galvanostatic mode with the voltage range of 3–5 V at a room temperature using a half-cell with a lithium anode and an electrolyte based on a 1 M  $\text{LiPF}_6$  solution in an ethylene carbonate and dimethyl carbonate mixture at a cycling rate equal to  $C/10$ , where  $C = 167 \text{ mA/g}$ .

## RESULTS AND DISCUSSION

Figure 1 demonstrates the diffraction patterns of the synthesized solid solutions  $\text{LiCo}_{1-y}\text{Fe}_y\text{PO}_4$  ( $0 \leq y \leq 1$ ). All samples are single-phase they crystallize in the rhombic system (sp. gr.  $Pnma$ ). The structure can be represented as a chain of octahedras  $\text{MO}_6$  ( $M = \text{Co}, \text{Fe}$ ) along the axis  $c$ , those are bound by the  $\text{PO}_4^{3-}$  tetrahedra which are linked to form a three-dimensional framework. The  $\text{MO}_6$  forming zigzag chains are interconnected by vertices rather than by faces, which hampers the electron transfer [16]. The diffusion of lithium ions is implemented through one-dimensional channels along the axis  $b$  (direction  $[010]$ ).

Figure 2 demonstrates the diffraction pattern for  $\text{LiCo}_{0.9}\text{Fe}_{0.1}\text{PO}_4$ , refined using a Rietveld

method, and Fig. 3 demonstrates unit cell parameters depending on the iron content. It can be seen that  $a$  and  $b$  parameters increase with Fe content in the samples, whereas the  $c$  parameter decreases. The anisotropic change in the parameters leads to an increase in the cell volume. The refined unit cell parameters for the samples synthesized depending on the content of Fe is in a good agreement with the data obtained by the authors of [8].

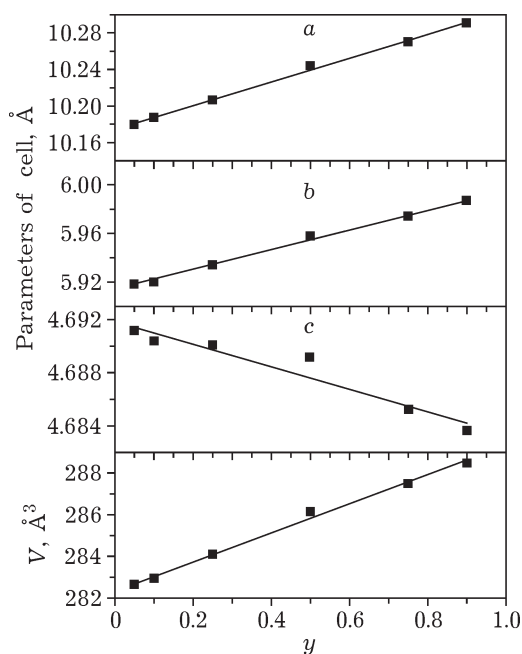


Fig. 3. Lattice parameters ( $a$ ,  $b$ ,  $c$ ) and unit cell volume ( $V$ ) for solid solutions  $\text{LiCo}_{1-y}\text{Fe}_y\text{PO}_4$  depending on composition parameter ( $y$ ).

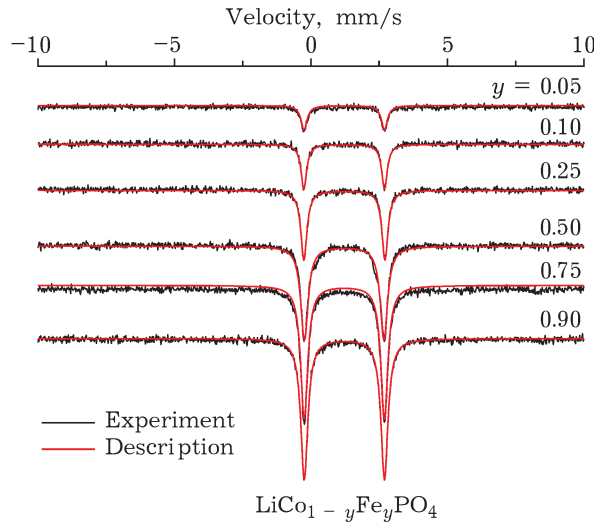


Fig. 4. Mössbauer spectra of  $\text{LiCo}_{1-y}\text{Fe}_y\text{PO}_4$  ( $0 \leq y \leq 1$ ) solid solutions.

The local structure of the solid solutions  $\text{LiCo}_{1-y}\text{Fe}_y\text{PO}_4$  ( $0 \leq y \leq 1$ ) synthesized was studied by means of NGR spectroscopy, which allows determining the electronic state of Fe ions in the material (Fig. 4). It is seen that all the spectra exhibit a doublet corresponding to  $\text{Fe}^{2+}$  ions in an octahedral environment, which is inherent in the structure of olivine [17]. No presence of any impurity phases was revealed. The doublet intensity exhibits an increase with increasing Fe content in the samples. Data concerning the width, chemical shift and quadrupole splitting in the NGR spectra are presented in Table 1.

According to the results of SEM, the primary particles of the synthesized  $\text{LiCoPO}_4$ ,  $\text{LiCo}_{0.5}\text{Fe}_{0.5}\text{PO}_4$  and  $\text{LiFePO}_4$  samples have a shape

TABLE 1

Width, chemical shift (CS), quadrupole splitting (QS) and the state of Fe ions in  $\text{LiCo}_{1-y}\text{Fe}_y\text{PO}_4$  ( $0 \leq y \leq 1$ ) solid solutions according to NGR spectroscopy. The content of  $\text{Fe}^{2+}$  is 100 %

$y$	Width, mm	QS, mm/s	IS, mm/s
0.05	0.26	2.95	1.22
0.10	0.25	2.96	1.22
0.25	0.27	2.97	1.23
0.50	0.33	2.91	1.22
0.75	0.31	2.94	1.22
0.90	0.31	2.94	1.23
1	0.37	2.95	1.22

close to spherical one, and the average size ranging from 200 to 250 nm (Fig. 5, *a-c*). The primary particles are combined into secondary loose agglomerates of 10–15  $\mu\text{m}$  in size. The chemical composition of synthesized solid solutions such as  $\text{LiCo}_{1-y}\text{Fe}_y\text{PO}_4$  ( $0 \leq y \leq 1$ ) was confirmed by means of energy dispersion energy-dispersive X-ray spectroscopy (EDX). Figure 5, *d* demonstrates an EDX spectrum of  $\text{LiCo}_{0.5}\text{Fe}_{0.5}\text{PO}_4$  sample.

It is known that the charge-discharge profiles of  $\text{LiFePO}_4$  and  $\text{LiCoPO}_4$  look like a plateau, which correlates with a two-phase mechanism of the intercalation/deintercalation of lithium ions [4, 18]. This means that at each point of the experimental curve the material exhibits two phases to be present therein such as the initial phase of  $\text{LiMPO}_4$  and the final phase of  $\text{MPO}_4$  ( $\text{M} = \text{Fe}, \text{Co}$ ). The plot of  $dQ/dU$  depending on the voltage demonstrates the pairs of corresponding redox peaks. The feature of  $\text{LiCoPO}_4$  consists in the fact that there are two oxidation peaks present, as opposed to one peak for  $\text{LiFePO}_4$ , which could be explained by the formation of an intermediate phase of  $\text{Li}_{0.7}\text{CoPO}_4$  in the course of charge process. However, the discharge of  $\text{LiCoPO}_4$  occurs in a single-stage manner with no formation of any intermediate phase.

Figure 6 demonstrates the charge-discharge profiles of the synthesized solid solutions  $\text{LiCo}_{1-y}\text{Fe}_y\text{PO}_4$  ( $0 \leq y \leq 1$ ) within the voltage range of 3–5 V at a rate of cycling equal to  $C/10$ . One can see that the curves exhibit two plateaus at 3.4 and 4.8 V. The first plateau at 3.4 V corresponds to a redox couple of  $\text{Fe}^{2+}/\text{Fe}^{3+}$ , whereas the second one (at 4.8 V) corresponds to a redox couple of  $\text{Co}^{2+}/\text{Co}^{3+}$ . The plots of  $dQ/dU$  depending on voltage exhibit present three oxidation and two reduction peaks (Fig. 7). From the data presented in Fig. 7 and Table 2 it follows that increasing the Fe content in the samples the potential of  $\text{Co}^{2+}/\text{Co}^{3+}$  couple results in a considerable shifting towards lower voltage values (from 4.92 V for  $\text{LiCoPO}_4$  to 4.69 V for the  $\text{LiCo}_{0.1}\text{Fe}_{0.9}\text{PO}_4$  composition), whereas the potential of the  $\text{Fe}^{2+}/\text{Fe}^{3+}$  couple almost does not changes. It should also be noted that the oxidation peak at 4.81 V, corresponding to the formation of an intermediate phase such as  $\text{Li}_{0.7}\text{CoPO}_4$  disappears in going to the composition of  $\text{LiCo}_{0.5}\text{Fe}_{0.5}\text{PO}_4$ . For the com-

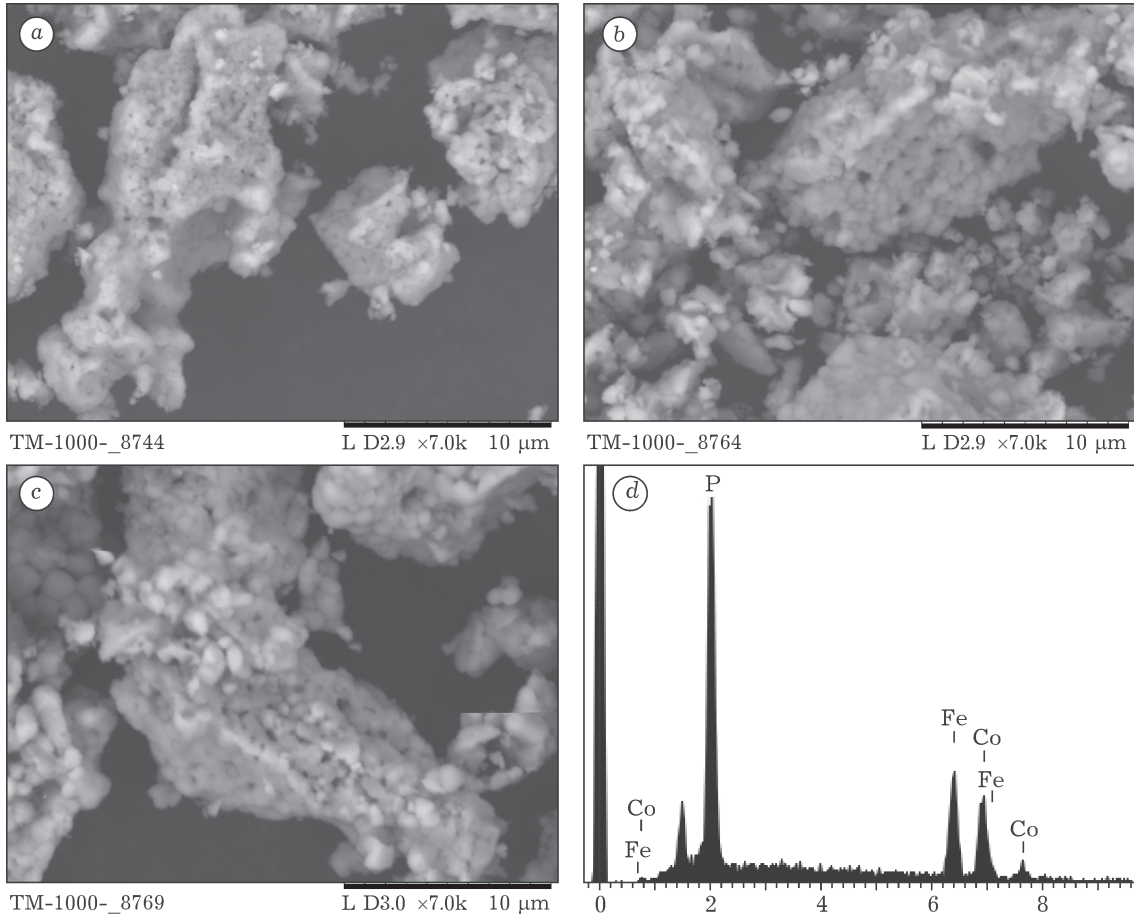


Fig. 5. Micrographs of  $\text{LiCoPO}_4$  (a),  $\text{LiCo}_{0.5}\text{Fe}_{0.5}\text{PO}_4$  (b),  $\text{LiFePO}_4$  (c) and EDX spectrum for  $\text{LiCo}_{0.5}\text{Fe}_{0.5}\text{PO}_4$  (d).

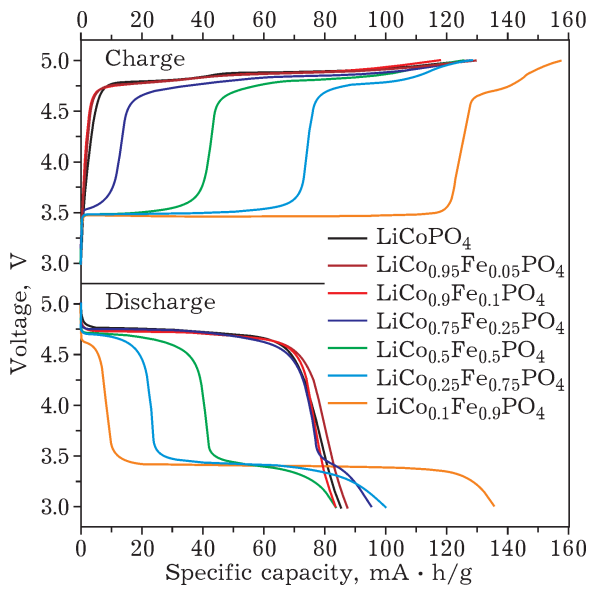


Fig. 6. Charge-discharge profiles for solid solutions  $\text{LiCo}_{1-y}\text{Fe}_y\text{PO}_4$  ( $0 \leq y \leq 1$ ).

positions with  $y \geq 0.5$  within the range of high voltage values, only one oxidation peak is observed, *i. e.* any intermediate phase, to all appearance, is not formed. To all appearance, this could be caused by changing the mechanism of lithium deintercalation from the single-phase mechanism to a two-phase mechanism, which

TABLE 2

Changing the  $\text{Fe}^{2+}/\text{Fe}^{3+}$  and  $\text{Co}^{2+}/\text{Co}^{3+}$  couple potential in the course of cycling  $\text{LiCo}_{1-y}\text{Fe}_y\text{PO}_4$  ( $0 \leq y \leq 1$ ), V

$y$	$\text{Fe}^{2+}/\text{Fe}^{3+}$		$\text{Co}^{2+}/\text{Co}^{3+}$		
	Charge	Discharge	Charge	Discharge	
0	—	—	4.81	4.92	4.72
0.05	—	—	4.77	4.87	4.72
0.10	—	—	4.77	4.87	4.72
0.25	3.54	3.42	4.74	4.84	4.74
0.50	3.49	3.40	—	4.80	4.71
0.75	3.49	3.42	—	4.77	4.70
0.90	3.47	3.40	—	4.69	4.61

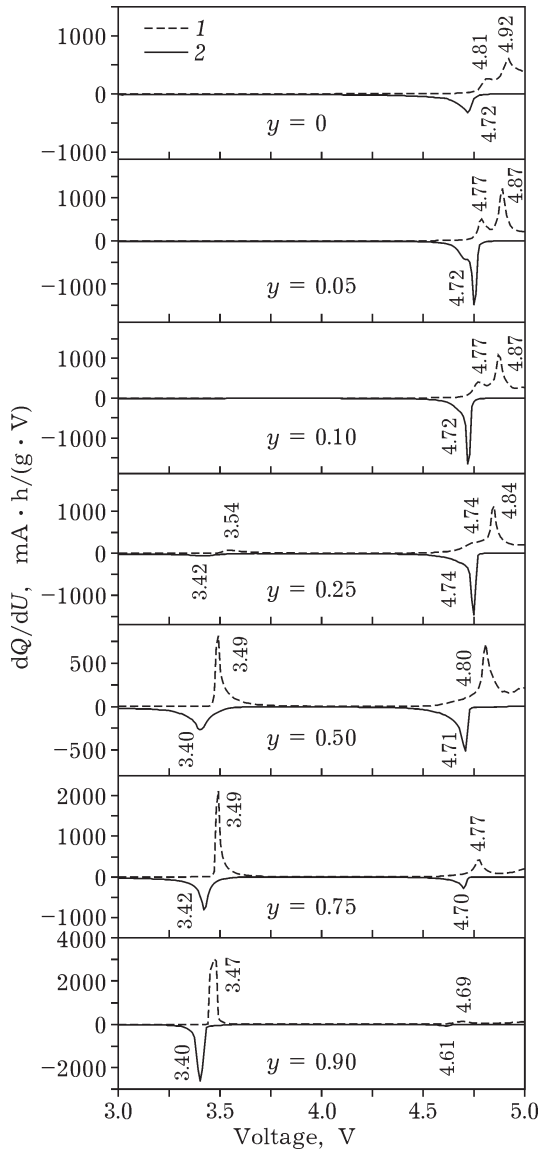


Fig. 7.  $dQ/dU$  depending on voltage for solid solutions  $\text{LiCo}_{1-y}\text{Fe}_y\text{PO}_4$  ( $0 \leq y \leq 1$ ): 1 – charge, 2 – discharge.

we observed earlier in the case of solid solutions  $\text{LiFe}_{1-y}\text{Mn}_y\text{PO}_4$  [19]. A significant shift in the  $\text{Co}^{2+}/\text{Co}^{3+}$  couple potential to lower voltage values allow one to perform cycling the cathode materials based on  $\text{LiCoPO}_4$  with the participation of  $\text{Co}^{2+}/\text{Co}^{3+}$  couple within the voltage range lower than 4.85 V, *i. e.*, with no going beyond the electrochemical window of the standard electrolyte [20, 21].

Changing the potential of the redox couple  $\text{Co}^{2+}/\text{Co}^{3+}$  in the course of cycling could be caused by a partial substitution of  $\text{Co}^{2+}$  by  $\text{Fe}^{2+}$  in the structure of  $\text{LiCoPO}_4$  to form solid solutions  $\text{LiCo}_{1-y}\text{Fe}_y\text{PO}_4$  as well as by some chang-

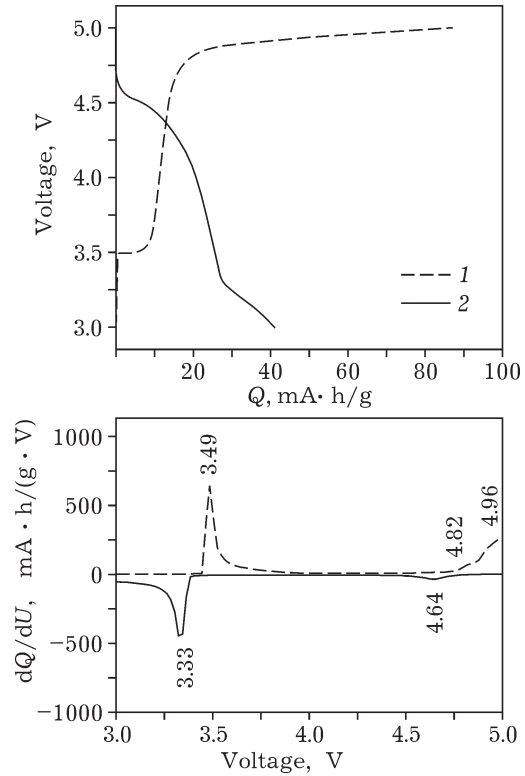


Fig. 8. Charge-discharge profile and  $dQ/dU$  depending on voltage for mechanical mixture  $0.9\text{LiCoPO}_4/0.1\text{LiFePO}_4$ : 1 – charge, 2 – discharge.

ing in the electronic structure thereof. This exhibits a distinction between solid solutions  $\text{LiCo}_{1-y}\text{Fe}_y\text{PO}_4$  and the mechanical mixtures of  $\text{LiCoPO}_4$  and  $\text{LiFePO}_4$  with a similar composition, for those such an effect is not observed. The charge-discharge profile and the  $dQ/dU$  voltage curve for the mechanical mixture

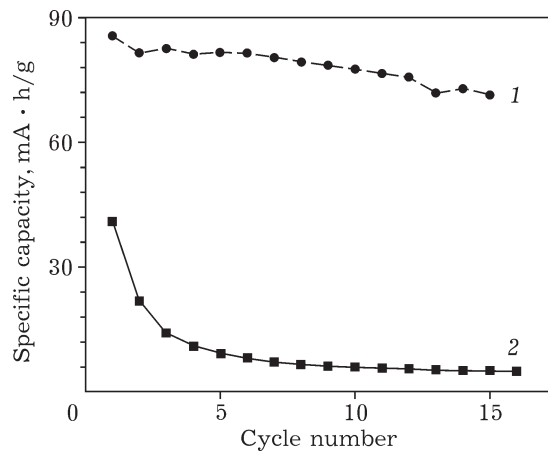


Fig. 9. Specific discharge capacity depending on the cycle number for the solid solution  $\text{LiCo}_{0.9}\text{Fe}_{0.1}\text{PO}_4$  (1) and mechanical mixture  $0.9\text{LiCoPO}_4/0.1\text{LiFePO}_4$  (2).

$0.9\text{LiCoPO}_4/0.1\text{LiFePO}_4$  (Fig. 8) demonstrate that the potential of the  $\text{Co}^{2+}/\text{Co}^{3+}$  couple does not change. The specific discharge capacity for the solid solution of  $\text{LiCo}_{0.9}\text{Fe}_{0.1}\text{PO}_4$  is to a significant extent higher than the specific capacity for the mechanical mixture of  $0.9\text{LiCoPO}_4$  and  $0.1\text{LiFePO}_4$ , both for the first, and for the subsequent cycles (Fig. 9).

## CONCLUSION

Thus, a simple mechanochemically stimulated solid-phase synthesis of single-phase highly dispersed solid solutions  $\text{LiCo}_{1-y}\text{Fe}_y\text{PO}_4$  ( $0 \leq y \leq 1$ ) has been implemented *via* carbothermal cobalt and iron oxide reduction. It has been demonstrated that all the samples crystallize in the orthorhombic system, space group *Pnma*, therewith the volume of the unit cell exhibits an increase with increasing the content of Fe. It has been found that increasing the Fe content in the samples results in the fact that  $\text{Co}^{2+}/\text{Co}^{3+}$  couple potential is markedly shifted to lower voltage values. Owing to this, the cathode materials based on  $\text{LiCoPO}_4$  could be used in rechargeable cells with a standard electrolyte.

## Acknowledgement

The authors express their gratitude to N. V. Bulina, V. R. Podugolnikov, S. A. Petrov and E. T. Devyatkina for assistance in conducting the investigations.

## REFERENCES

- 1 Hu M., Pang X., Zhou Z., *J. Power Sources*, 237 (2013) 229.
- 2 Padhi A. K., Nanjundaswamy K. S., Goodenough J. B., *J. Electrochem. Soc.*, 144 (1997) 1188.
- 3 Sharabi R., Markevich E., Borgel V., Salitra G., Aurbach D., Semrau G., Schmidt M. A., Schall N., Stinner C., *Electrochem. Commun.*, 13 (2011) 800.
- 4 Bramnik N. N., Nikolowski K., Baecht C., Bramnik K. G., Ehrenberg H., *Chem. Mater.*, 19 (2007) 908.
- 5 Wolfenstine J., *J. Power Sources*, 158 (2006) 1431.
- 6 Satya Kishore M. V. V. M., Varadaraju U. V., *Mater. Res. Bull.*, 40 (2005) 1705.
- 7 Kosova N. V., Devyatkina E. T., Slobodyuk A. B., Petrov S. A., *Electrochim. Acta*, 59 (2012) 404.
- 8 Neiton A., Thomas J. O., *Solid State Ionics*, 177 (2006) 1327.
- 9 Wang D., Wang Z., Huang X., Chen L., *J. Power Sources*, 146 (2005) 580.
- 10 Han D. W., Kang Y. M., Yin R. Z., Song M. S., Kwon H. S., *Electrochem. Commun.*, 11 (2009) 137.
- 11 Allen J. L., Jow T. R., Wolfenstine J., *J. Power Source*, 196 (2011) 8656.
- 12 Yang J., Xu J. J., *J. Electrochem. Soc.*, 153 (2006) 716.
- 13 Huang X., Ma J., Wu P., Hu Y., Dai J., Zhu Z., Chen H., Wang H., *Mater. Lett.*, 59 (2005) 578.
- 14 Kosova N., Devyatkina E., *Solid State Ionics*, 172 (2004) 181.
- 15 Toby B. H., *J. Appl. Cryst.*, 34 (2001) 210.
- 16 Amine K., Yasuda H., Yamachi M., *Electrochem. Solid-State Lett.*, 3(4) (2000) 178.
- 17 Yamada A., Kudo Y., Liu K. Y., *J. Electrochem. Soc.*, 148 (2001) A1153.
- 18 Kobayashi G., Nishimura S. I., Park M. S., Kanno R., Yashima M., Ida T., Yamada A., *Adv. Funct. Mater.*, 19 (2009) 395.
- 19 Kosova N. V., Devyatkina E. T., Ancharov A. I., Markov A. V., Karnaushenko D. D., Makukha V. K., *Solid State Ionics*, 225 (2012) 564.
- 20 Osnis A., Kosa M., Aurbach D., Major D. T., *J. Phys. Chem. C*, 117 (2013) 17919.
- 21 Muraliganth T., Manthiram A., *J. Phys. Chem. C*, 114 (2010) 15530.